Journal of Alloys and Compounds 520 (2012) 164–169

Contents lists available at SciVerse ScienceDirect

Journal of Alloys and Compounds

journal homepage: www.elsevier.com/locate/jallcom

Investigation of various reactions for the direct synthesis of $TiCr_2$ intermetallic compound from the TiO_2–Cr_2O_3–Ca system

O. Bayat*, A.R. Khavandi, R. Ghasemzadeh

School of Metallurgy and Materials Engineering, Iran University of Science and Technology, IUST, Tehran 16846-13114, Iran

ARTICLE INFO

Article history:
Received 22 July 2011
Accepted 30 December 2011
Available online 10 January 2012

Keywords:
Thermal analysis
Intermetallics
Hydrogen absorbing materials
X-ray diffraction

ABSTRACT

A new processing route was applied for the synthesis of $TiCr_2$ intermetallic powder directly by the Calciothermic co-reduction of TiO_2–Cr_2O_3 oxides. Differential thermal analysis (DTA) and X-ray diffraction (XRD) were used to determine the various reactions. According to DTA results heating the mixture up to about 675 °C resulted in an endothermic peak. This endothermic peak indicates the formation of a solid solution formation by the reaction of TiO_2 with Cr_2O_3. As the temperature increased to about 950 °C the Ca started to melt (at approximately 847 °C) resulting to an exothermic peak due to the reaction of Ca with Cr_2O_3 forming Cr metal. The formation of $CaTiO_3$ formed by the reaction of CaO with TiO_2 decreased the amount of TiO_2 in the mixture of starting materials. When the mixture was heated up to 1058 °C, Ca reacted with TiO_2 forming Ti as indicated by an exothermic reaction forming Ti. Finally, when the holding time at 1200 °C and the amount of Ca were increased, the $TiCr_2$ intermetallic was formed while the $CaTiO_3$ compound was gradually disintegrated into CaO and Ti and the amount of oxygen content in samples was decreased. The obtained intermetallic powder showed the capability of hydrogen storage after being activated.

1. Introduction

Nowadays the development of efficient and energy-saving technologies is of great importance. Calciothermic co-reduction and simultaneous synthesizing are novel and simple methods for making certain ceramics, intermetallic compounds and composites [1–7].

$TiCr_2$, as an intermetallic compound, can absorb hydrogen under high pressure at room temperature. Ti–Cr-based alloys have been developed in order to improve the hydrogen properties and surface sensitivity [8–13], more specifically, Ti–57.5Cr–5V alloy can absorb/desorb about 2.8% mass hydrogen at 313 K [14].

In the industrial production of these alloys, Ti is usually extracted through the Kroll process in which titanium tetrachloride is reduced by magnesium in order to form a titanium sponge and magnesium chloride and Cr is extracted by electrolysis or reduced by either Al or Si [15]. To prepare alloys, these elemental metals are arc-melted several times and heated for homogenization and pulverized. This long process consumes a lot of thermal and chemical energy, which can turn to a barrier for the mass production of these alloys. Calciothermic co-reduction is reported as a new and successful method for the production of TiAl, TiV, TiNbTaZr, Nb–FeB, Sm–Co and Nb–Ta alloys. Previous studies were focused on the in situ dissolution or electrolysis of the CaO by-product in the molten salt, molar ratio of the molten salt and electrolysis parameters of the synthesized compounds requiring long times up to 84.4 ks [16–22].

This research is designed for the direct synthesis of $TiCr_2$ intermetallic powder by the Calciothermic co-reduction of its oxides according to the following reaction:

$$TiO_2 + Cr_2O_3 + 5Ca = TiCr_2 + 5CaO \quad (1)$$

In this article, the various reactions in the TiO_2–Cr_2O_3–Ca system are investigated by means of differential thermal analysis (DTA) and subsequent X-ray diffraction (XRD) analysis according to the following reaction schemes:

$$TiO_2 + 2Ca = Ti + 2CaO \quad (2)$$

$$Cr_2O_3 + 3Ca = 2Cr + 3CaO \quad (3)$$

$$Ti + 2Cr = TiCr_2 \quad (4)$$

Identifying the effective parameters is very important for the schematization of mass production and this can be done by DTA surveys. The information obtained by DTA can be used for optimizing the production conditions and to have a better program.

The structure, elemental distribution and hydrogen property of the obtained samples were analyzed to confirm the success of the alloy's reduction.

* Corresponding author. Tel.: +98 21 77459151; fax: +98 21 77240480.
E-mail addresses: obayat@iust.ac.ir (O. Bayat), khavandi@iust.ac.ir (A.R. Khavandi), rhzadeh@iust.ac.ir (R. Ghasemzadeh).

0925-8388/$ – see front matter © 2012 Elsevier B.V. All rights reserved.
doi:10.1016/j.jallcom.2011.12.174

Table 1
Green mixtures used in DTA experiments.

Exp. run	Amount, mol			Holding time (min) at 1200 °C
	TiO_2	Cr_2O_3	*Ca*	
1	1	–	2	30–60
2	1	–	2.5	30–60
3	1	–	3	30–60
4	–	1	3	30–60
5	–	1	3.5	30–60
6	–	1	4	30–60
7	1	1	6.5	30–60
8	1	1	7	30–60–120
9	–	–	1	–

2. Materials and methods

The raw materials used are TiO_2 (Merck, 99.9%), Cr_2O_3 (Merck, 99.9%), and Ca (Merck, 99.7%).

DTA was used (heating rate of 20° min^{-1}, up to 1200 °C) with a duration time of 30 and 60 min in order to investigate on the reaction steps of the combustion synthesis. The starting mixtures used in these experiments are characterized in Table 1. For accurate investigation on the reactions and products of the TiO_2–Cr_2O_3–Ca system, the TiO_2–Ca and Cr_2O_3–Ca systems were also investigated as can be seen in Table 1.

For each experiment, green mixtures were milled in a high-energy planetary ball mill (model Fritsch P6) using WC vial and balls in highly pure Argon for 20 min.

DTA measurements were done with approximately 400 mg and heated under static pressure of high-purity argon gas. In order to obtain enough material, each experiment was carried out 4–5 times. The materials formed in the DTA device were characterized by XRD (Seifert 3003TT, Cu-K_α radiation), scanning electron microscope (SEM) (Vega©Tescan) and energy dispersive spectroscopy (EDS).

For comparison of properties a sample was prepared by arc-melting on a water-cooled copper hearth under the pure Argon atmosphere from pure Ti and Cr elements. This sample was re-melted 4 times to ensure its homogeneity.

The hydrogen activation and kinetics of the obtained powders (arc-melt and Calciothermic reduction powders) were characterized by Sievert's method. The samples were annealed at 560 °C for 12 h under vacuum and subsequently activated at 300 °C under 2.5 MPa hydrogen pressure. Kinetic measurements were performed at 50 °C under 2.5 MPa and 0.005 MPa of hydrogen pressures for absorption and desorption, respectively. These experimental conditions were similar to the ones used by Hu et al. [12].

3. Results and discussion

For accurate investigation on the formation mechanism, DTA and XRD experiments were applied separately on the TiO_2–Ca and Cr_2O_3–Ca systems.

3.1. TiO_2–Ca system

The DTA results of this system (mixture of TiO_2 and Ca) are shown in Fig. 1(a). According to Fig. 1(a) three peaks can be observed, two endothermic peaks at 457 and 847 °C and one exothermic peak at 1058 °C. According to the DTA of Ca in Fig. 1(b), the two endothermic peaks observed correspond to the $\alpha \rightarrow \beta$ phase transformation and melting of Ca, respectively [23]. The exothermic peak at 1058 °C corresponds to the reaction between TiO_2 and Ca. The XRD patterns of the material formed upon heating TiO_2 and Ca up to 1200 °C are shown in Fig. 2.

According to Fig. 2, under reduction conditions of Ca = 2 (molar ratio) at holding time of 30 min, the spinal compound, $CaTiO_3$, was produced by the reaction of CaO (by-product) with the starting TiO_2 powder after some time delay. Due to the higher stability of $CaTiO_3$ compared to TiO_2, the reduction of $CaTiO_3$ is difficult and requires more time.

As can be seen in Fig. 2, at Ca = 2 (molar ratio) and t = 60 min, CaO and $TiO_{0.325}$ are present while the smaller intensity of $CaTiO_3$ peaks indicate the dissection of $CaTiO_3$ to CaO and $TiO_{0.325}$.

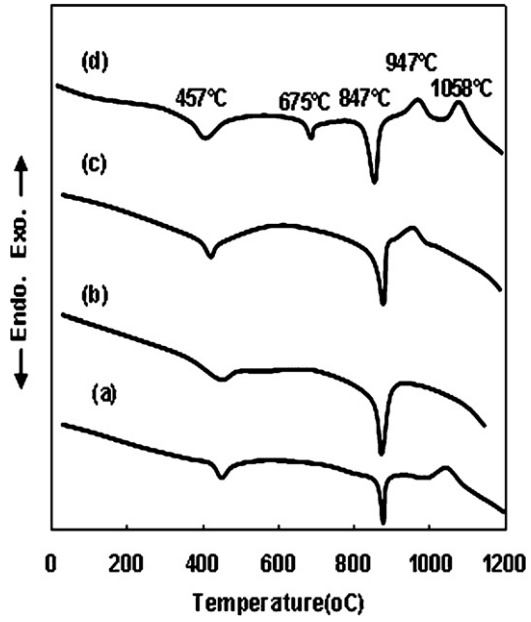

Fig. 1. DTA curves of different systems: (a) TiO_2–Ca, (b) Ca, (c) Cr_2O_3–Ca and (d) TiO_2–Cr_2O_3–Ca.

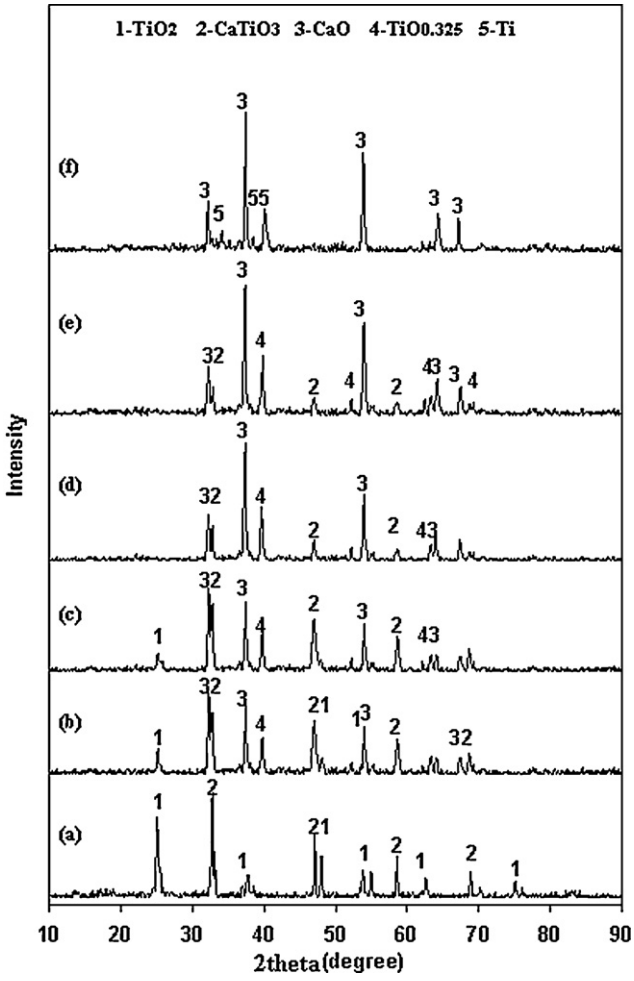

Fig. 2. X-ray patterns of the DTA products in the TiO_2–Ca systems: (a) Ca = 2 (molar ratio), t = 30 min (holding time at 1200 °C), (b) Ca = 2, t = 60 min, (c) Ca = 2.5, t = 30 min, (d) Ca = 2.5, t = 60 min, (e) Ca = 3 and t = 30 min and (f) Ca = 3, t = 60 min.

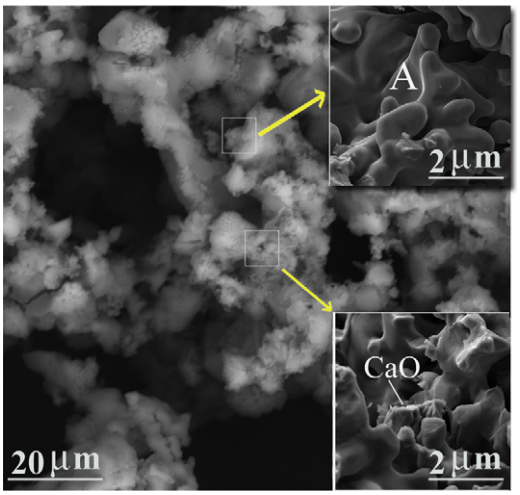

Fig. 3. SEM image of Ti obtained at Ca = 3 and t = 60 min.

However, Ca was not observed due to evaporation indicating that it was not sufficient for the reduction.

At t = 30 min and Ca = 2.5 (molar ratio), the obtained XRD pattern was similar to the one obtained at t = 60 min and Ca = 2 (mol ratio) (Fig. 2); with higher intensity of $CaTiO_3$ peaks. By increasing the time (from 30 to 60 min), the TiO_2 starting material disappeared and the amount of $TiO_{0.325}$ increased; while Ca was not observed.

At t = 30 min and Ca = 3 (molar ratio), the TiO_2 starting material disappeared while CaO was the main phase (Fig. 2). By increasing the time (60 min), Ti peaks were observed along with very low intensity peaks of $CaTiO_3$. In other words, the prolonged reaction time decreased the amount of $CaTiO_3$ and reduced it to Ti and CaO. Peaks of Ca were not observed due to the evaporation during the process. In order to completely eliminate the TiO_2, evaporation of Ca must be prevented. Also, the minimum required time for the Calciothermic reduction of TiO_2 is 60 min.

Fig. 3 shows the SEM micrograph of products formed in the reaction of TiO_2–Ca mixture obtained for t = 60 min and Ca = 3 (molar ratio) after leaching. By investigating these results, it can be found that Ti metal can be produced with particle sizes of 5–20 μm along with amounts of CaO particles captured in the particles (marked in Fig. 3). As can be seen in Fig. 3, some Ti particles sinter and coalesce into larger particles (marked as A) at the reduction reaction temperature.

3.2. Cr_2O_3–Ca system

DTA results of this system (the mixture of Cr_2O_3 and Ca) are shown in Fig. 1(c). It is evident in Fig. 1(c) that there are three peaks (two endothermic peaks at 457 and 847 °C and one exothermic peak at 947 °C) in these results. As explained before, two endothermic peaks correspond to the phase transformation and the melting of Ca. The exothermic peak at 947 °C corresponds to the reaction between Cr_2O_3 and Ca. The XRD patterns of the material formed upon heating Cr_2O_3 and Ca up to 1200 °C are shown in Fig. 4.

At t = 30 min and Ca = 3 (molar ratio), $CaCr_2O_4$ was found, which indicates that CaO (by-product) reacted with the Cr_2O_3 starting material in order to form $CaCr_2O_4$. According to the binary phase diagram of CaO–Cr_2O_3, $CaCr_2O_4$ is stable below 900 °C and has a large confinement up to 40 mol% CaO [25]. By increasing the holding time (from 30 to 60 min), the peaks corresponding to Cr_2O_3 disappear and Cr metal and CaO are formed.

As is shown in Fig. 4, at t = 30 min and Ca = 3.5 (molar ratio), the XRD pattern and products are similar to t = 60 min and Ca = 3 (molar ratio). Although by increasing the holding time to 60 min,

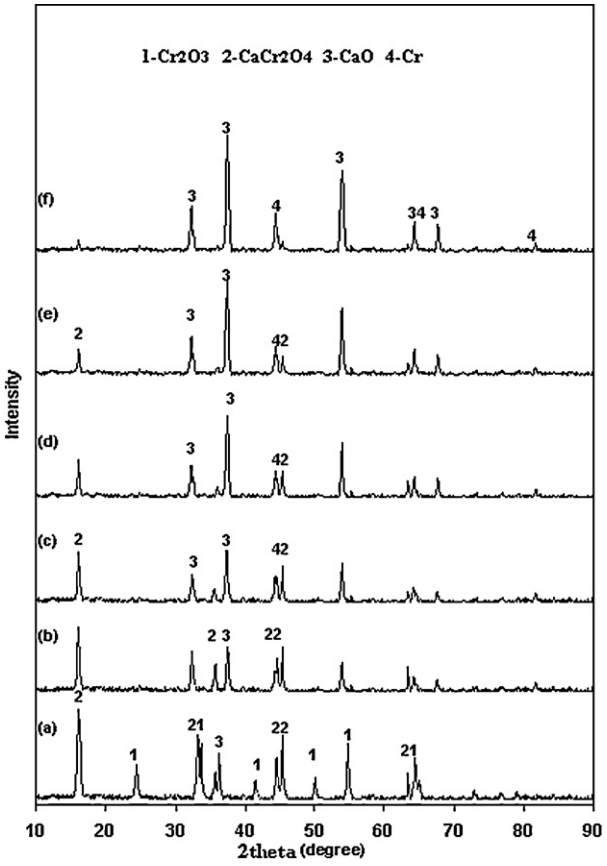

Fig. 4. X-ray patterns of the DTA products in the Cr_2O_3–Ca systems: (a) Ca = 3 (molar ratio), t = 30 min (holding time at 1200 °C), (b) Ca = 3, t = 60 min, (c) Ca = 3.5, t = 30 min, (d) Ca = 3.5, t = 60 min, (e) Ca = 4 and t = 30 min and (f) Ca = 4, t = 60 min.

the intensity of CaO and Cr peaks increase, which indicates that the disintegration of $CaCr_2O_4$ is in progress. The peaks of Ca were not observed at this stage indicating that the amount of Ca was not enough.

At t = 30 min and Ca = 4 (molar ratio), the intensity of $CaCr_2O_4$ was less and by increasing the holding time to 60 min, it disappeared. Therefore, the reduction of Cr_2O_3 was completed at this condition.

Fig. 5 shows the SEM micrograph of the products formed in the reaction of Cr_2O_3–Ca mixture at t = 60 min and Ca = 4 (molar ratio) after leaching the DTA products. It can be seen that Cr metal can be produced with particle sizes of about 10–20 μm. The marked difference in the size of the powders can be attributed to the higher melting point of Cr (1866 °C) in comparison with that of Ti (1668 °C).

3.3. TiO_2–Cr_2O_3–Ca system

Due to the evaporation of Ca during the reduction process, the mixture of TiO_2–Cr_2O_3 was heated with Ca = 6.5 and 7 (molar ratio). DTA curves are shown in Fig. 1(d). According to these results, three endothermic peaks are seen at 457, 675 and 847 °C. Two peaks at 457 and 847 °C correspond to the phase transformation and Ca melting, respectively (as mentioned in Section 3.1).

The main difference in the DTA results was revealed at the 675 °C when the TiO_2–Cr_2O_3–Ca system (Fig. 1(d)) was compared with the TiO_2–Ca and Cr_2O_3–Ca systems (Fig. 1(a and c). At this temperature, no reaction is observed between Ca on the one hand and TiO_2 or Cr_2O_3 on the other hand, therefore it seems that an endothermic reaction occurs between TiO_2 and Cr_2O_3. To prove this fact, the mixture of TiO_2–Cr_2O_3 with a molar ratio of 1:1 was prepared. The

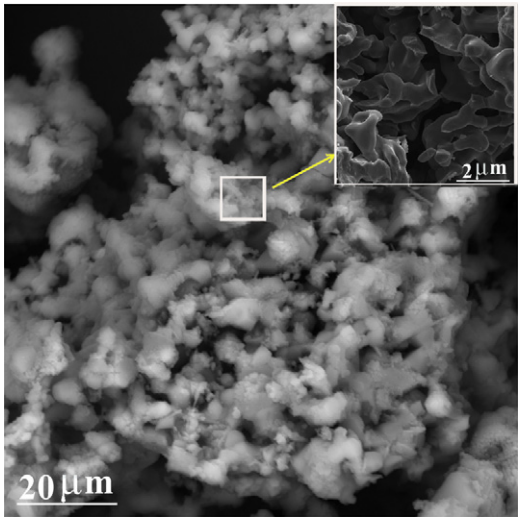

Fig. 5. SEM image of Cr obtained at Ca = 4 and t = 60 min.

mixture was charged into a WC vial with WC balls under a high-purity Argon atmosphere and milled for 20 min and subsequently it was heated up to 750 °C for 30 min. Fig. 6 shows the XRD pattern of products. According to the TiO_2–Cr_2O_3 phase diagram [24], these two oxides form a solid solution and Cr_2O_3 at 750 °C. As can been seen in Fig. 6, XRD results show the presence of the starting materials (TiO_2) indicating that the time of the process was not enough for the complete formation of the solid solution.

According to the DTA data (Fig. 1), after the melting of Ca, two exothermic peaks are seen at 947 and 1058 °C. A review of the TiO_2–Ca (Fig. 1(a)) and Cr_2O_3–Ca (Fig. 1(c)) systems reveal that these peaks correspond to the reaction between the melting of Ca, Cr_2O_3 and TiO_2, respectively.

Fig. 7 shows the XRD results of the reduced samples obtained from the DTA experiments. At Ca = 6.5 (molar ratio) and t = 30 min, $CaTiO_3$, CaO and Cr were present. As shown in Fig. 7, $CaTiO_3$ is the main phase and by increasing the time (from 30 to 60 min), the intensity of CaO peaks increase and $TiO_{0.325}$ is formed. This means that the prolonged reaction could decrease the amount of $CaTiO_3$ and reduce it to CaO and Ti.

At the reduction condition t = 60 min and Ca = 7 (molar ratio), the XRD pattern was similar to t = 60 min and Ca = 6.5 (molar ratio) (Fig. 7b and c). The higher the intensity of the CaO peaks, the more the dissection of $CaTiO_3$. By increasing the time to 60 min, the Ti and Cr metals were formed while the intensity of the $TiCr_2$ intermetallic peaks was very weak. As shown in Fig. 6 the $TiCr_2$ compound

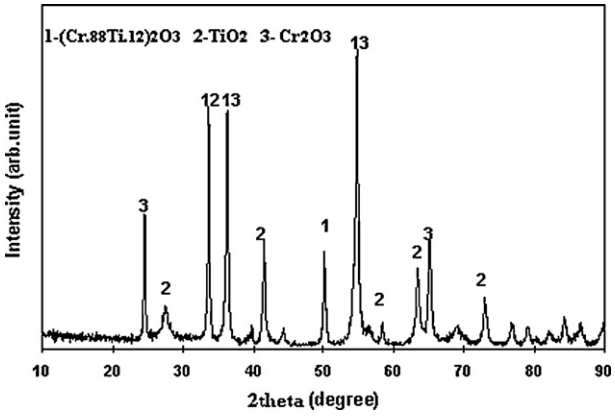

Fig. 6. X-ray patterns of the material formed during TiO_2–Cr_2O_3 heated at 750 °C and 30 min.

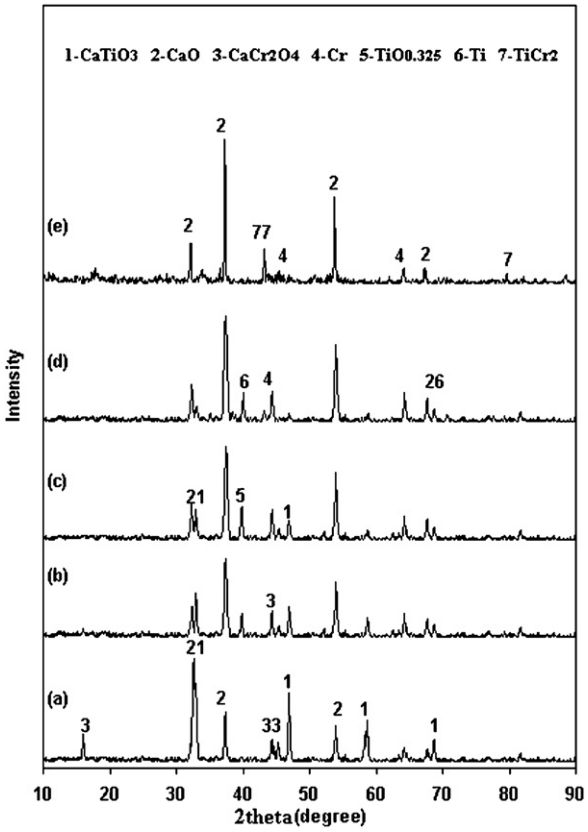

Fig. 7. X-ray patterns of the DTA products in the TiO_2–Cr_2O_3–Ca systems: (a) Ca = 6.5 (molar ratio), t = 30 min (holding time at 1200 °C), (b) Ca = 6.5, t = 60 min, (c) Ca = 7, t = 30 min, (d) Ca = 7, t = 60 min and (e) Ca = 7 and t = 120 min.

appeared by increasing the holding time to 120 min. This implies that the formation of $TiCr_2$ intermetallic is a diffusion process and needs more time at the elevated temperature.

SEM and EDS results of the products at t = 60 min and Ca = 7 (molar ratio) are shown in Fig. 8. The results show that most particles are pure Ti and Cr. As be shown in Fig. 8 a small particle of Ti was isolated from the grains (marked as A), which might be formed from the $CaTiO_3$. EDS analyses (Fig. 8) indicated that at the interface of the Ti and Cr particles, Ti–Cr alloy was formed, which

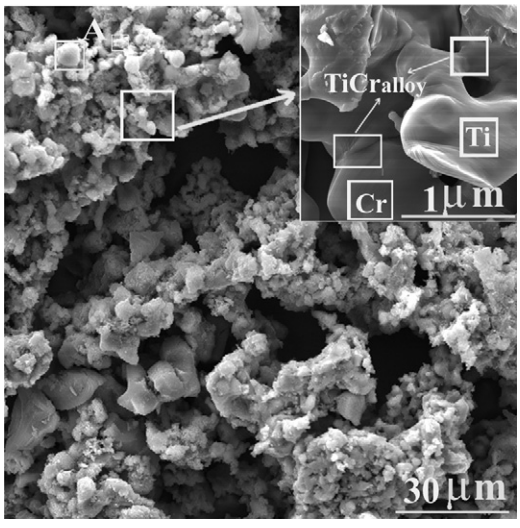

Fig. 8. SEM image of Ti–Cr obtained at Ca = 7 and t = 60 min and EDS analysis of particles.

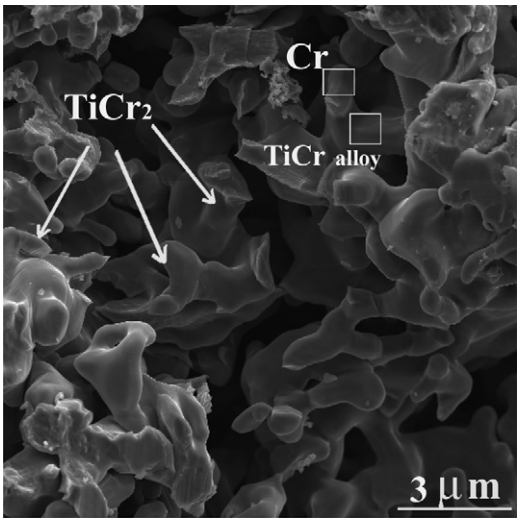

Fig. 9. SEM image of Ti–Cr obtained at Ca = 7 and t = 120 min.

implies that the formation of $TiCr_2$ compound is a mutual diffusion process.

Fig. 9 shows the SEM micrograph of the products at t = 120 min and Ca = 7 (molar ratio). The averaged concentration by EDS was in agreement with the target concentration and most particles were consistent with the composition of α-$TiCr_2$. According to the Ti–Cr phase diagram [25], the α-$TiCr_2$ compound is stable at room temperature and contains 64 wt% Cr also β-$TiCr_2$ is stable at high temperatures containing about 66 wt% Cr. In equilibrium conditions and at 1200 °C, two phases are stable, β-$TiCr_2$ and β solid solution. β-$TiCr_2$ transformed to α-$TiCr_2$ and β-solid solution at 850 °C by cooling. However, the concentrations of some particles were analyzed as a Ti–Cr solid solution, which indicates that the diffusion after co-reduction or the decomposition product from β-$TiCr_2$ was not sufficient. This means that the time of reaction is not enough for the diffusion of elements in order to form $TiCr_2$, or the local heterogeneity of the compound caused space between particles and, therefore, the time of reduction must be increased.

3.4. Oxygen concentration

The samples were washed with distilled water several times and then leached by a 10 vol% HCl solution to remove the by-products. Finally the powders were dried under vacuum. The oxygen content of the samples was analyzed by the inert gas fusion – infrared absorption method (LECO TC600) (Table 2).

The amount of oxygen in initial starting mixture was about 35% mass, but, in the products, this amount had a sharp decrease. However, the thermodynamic equilibrium oxygen content at 1200 K is evaluated as about 500 ppm in Ti and less than 1 ppm in Cr under Ca/CaO equilibrium. In practice, these values are less than the theoretical values as shown in Table 2. The reason is that the holding time of process was not enough in the systems resulting in uncompleted synthesis. CaO was captured in the grain boundaries of the product during sintering which was hardly removed by acid leaching and also the amount of Ca was not enough since it evaporated during the process.

Table 2
Oxygen content in various metal products at different conditions.

Reaction conditions (mixture, time of process)	Product	Oxygen (ppm)
TiO_2 + 3Ca, t = 60 min.	Ti	1650
Cr_2O_3 + 4Ca, t = 30 min.	Cr	32
Cr_2O_3 + 4Ca, t = 60 min.	Cr	20
TiO_2 + Cr_2O_3 + 7Ca, t = 120 min	$TiCr_2$	1320

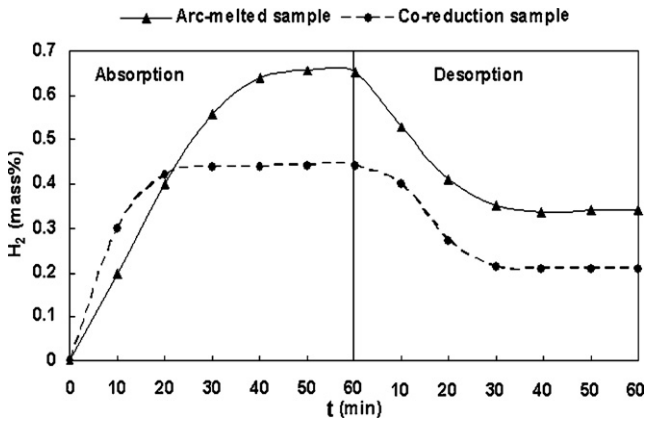

Fig. 10. Hydrogen adsorption–desorption capacities and kinetics of the co-reduced and arc-melted $TiCr_2$ at 50 °C.

As is shown in Table 2, the oxygen content in pure Cr decreased from 32 to 20 ppm by increasing the holding time from 30 to 60 min. The oxygen content in the $TiCr_2$ compound was also less than that the total oxygen content in the pure Ti and Cr, which was caused by increasing the holding time (from 60 to 120 min).

Suzuki and Inoue [26] reported that at the best condition less than 1000 ppm oxygen remained in the Ti powder when pure TiO_2 was reduced in the $CaCl_2$ by Ca. It is expected that the oxygen content in this work can be decreased by finding the optimum condition for the holding time at the elevated temperature and the optimum amount of Ca.

3.5. Hydrogen sorption properties

Activation treatment (see Section 2) was applied prior to the hydrogen property measurements to remove the oxide or organic layer contaminates generally formed at the surface of the samples.

Fig. 10 shows the hydrogen adsorption and desorption capacities and kinetics for arc-melting and co-reduction of $TiCr_2$ alloys at 50 °C. It can be seen that both co-reduced and arc-melted $TiCr_2$ can adsorb an amount of hydrogen. The maximum hydrogen adsorped for the arc-melted and co-reduced samples under 2.5 MPa hydrogen pressure are 0.65 and 0.44 wt%, respectively, while for hydrogen desorption they are 0.34 and 0.23 wt%, respectively. This discrepancy is due to different production processes. The arc-melted samples contain α and β-$TiCr_2$ phases since the solidification rate is very high in the water-cooled copper mould; the amount of oxygen concentration of the co-reduced sample is also high (Table 2). Therefore, hydrogen adsorption decreases in this sample [27].

The kinetic adsorption of the co-reduced sample is better than that of the arc-melted one due to the morphology and high surface area of this sample as can be seen in Fig. 8. This morphology is suitable for hydrogen adsorption [18].

4. Conclusions

Calciothermic co-reduction was used as a new method in order to synthesize $TiCr_2$ intermetallic powder directly from the oxide mixture of TiO_2 and Cr_2O_3. DTA and XRD results showed an exothermic reaction at about 947 °C between Ca and Cr_2O_3 forming Cr metal. When the mixture was heated up to 1058 °C, Ca reacted with TiO_2 by an exothermic reaction leading to the formation of Ti. Increase in the holding time of the mixture and the amount of Ca, gradually disintegrated the $CaTiO_3$ compound into CaO and

Ti. EDS analyses indicated that the formation of $TiCr_2$ compound is a mutual diffusion process that needs time for its formation. The activated powder showed capability as a hydrogen absorption material.

References

[1] R.W. Cahn, Non-Equlibrium Processing of Materials, Pergamon, 1999 (chapter 11), pp. 298–309.
[2] S. Gennari, F. Maglia, G. Spinolo, Intermetallics 11 (2003) 1355–1359.
[3] V. Rosenband, M. Torkar, A. Gany, Intermetallics 14 (2006) 551–559.
[4] A.G. Merzhanov, J. Mater. Process. Technol. 56 (1996) 222–241.
[5] A.G. Merzhanov, Ceram. Int. 21 (1995) 371–379.
[6] P. Mossino, Ceram. Int. 30 (2004) 311–332.
[7] J.J. Moore, H.J. Feng, Combustion Synthesis of Advanced Materials, Pergamon, 1995, pp. 275–316.
[8] S.W. Cho, C.N. Park, J.H. Yoo, J. Alloys Compd. 403 (2005) 262–266.
[9] S.W. Cho, C.N. Park, E. Akiba, J. Alloys Compd. 288 (1999) 294–298.
[10] H.C. Lin, K.M. Lin, K.C. Wu, Int. J. of Hydrogen Energy 32 (2007) 4966–4972.
[11] H. Taizhong, W. Zhu, X. Baojia, Mater. Chem. Phys. 93 (2005) 544–547.
[12] Y.Q. Hu, H.F. Zhang, C. Yan, L. Ye, Mater. Lett. 58 (2004) 783–786.
[13] S. Amira, S.F. Santos, J. Huot, Intermetallics 18 (2010) 140–144.
[14] M. Okada, T. Kuriiwa, T. Tamura, H. Takamura, A. Kamegawa, J. Alloys Compd. 330–332 (2002) 511–516.
[15] A.N. Zelikman, O.E. Krein, G.V. Samosonov, Metallurgy of Rare Metals, second ed., 1964.
[16] R.O. Suzuki, M. Ikwzawa, T.H. Okabe, T. Oishi, K. Ono, Mater. Trans. 31 (1) (1990) 61–68.
[17] R.O. Suzuki, T. Ueki, M. Ikwzawa, T.H. Okabe, T. Oishi, K. Ono, Mater. Trans. 32 (3) (1991) 272–277.
[18] R.O. Suzuki, K. Tatemoto, H. Kitagawa, J. Alloys Compd. 385 (2004) 173–180.
[19] Sh. Osaki, H. Sakai, R.O. Suzuki, J. Electrochem. Soc. 157 (8) (2010) 117–121.
[20] M. Steinhorst, J. Alloys Compd. 186 (1992) 177–185.
[21] H.G. Domazer, German Patent, 2303697 (1973).
[22] M. Baba, Y. Ono, R.O. Suzuki, J. Phys. Chem. Solids 66 (2005) 466–470.
[23] O. Kubaschewski, C.B. Alcock, Metallurgical Thermochemistry, 5th ed., Pergamon Press, 1979.
[24] American Ceramic Society, NIST, Phase Equilibria Diagrams Version 3.1, 2004.
[25] H. Okamoto, Phase Diagrams for Binary Alloys, ASM International, 2000.
[26] R.O. Suzuki, Sh. Inoue, Metall. Mater. Trans. B 34 (2003) 277–285.
[27] X. Liu, L. Jiang, Z. Li, Z. Huang, Sh. Wang, J. Alloys Compd. (2008).